

锐钛矿型 TiO₂ 负载的 Pd 催化剂用于乙炔选择加氢的催化性能及其表征

高晓平^{1,2} 郭章龙^{1,2} 周亚男^{1,2} 敬方梨¹ 储伟^{1,2,*}

(¹四川大学化学工程学院, 成都 610065; ²四川大学新能源与低碳技术研究院, 成都 610207)

Catalytic Performance and Characterization of Anatase TiO₂ Supported Pd Catalysts for the Selective Hydrogenation of Acetylene

GAO Xiao-Ping^{1,2} GUO Zhang-Long^{1,2} ZHOU Ya-Nan^{1,2} JING Fang-Li¹

CHU Wei^{1,2,*}

(¹School of Chemical Engineering, Sichuan University, Chengdu 610065, P. R. China; ²Institute of New Energy and Low-Carbon Technology, Sichuan University, Chengdu 610207, P. R. China)

*Corresponding author. Email: chuwei1965@scu.edu.cn; Tel: +86-28-85403836.

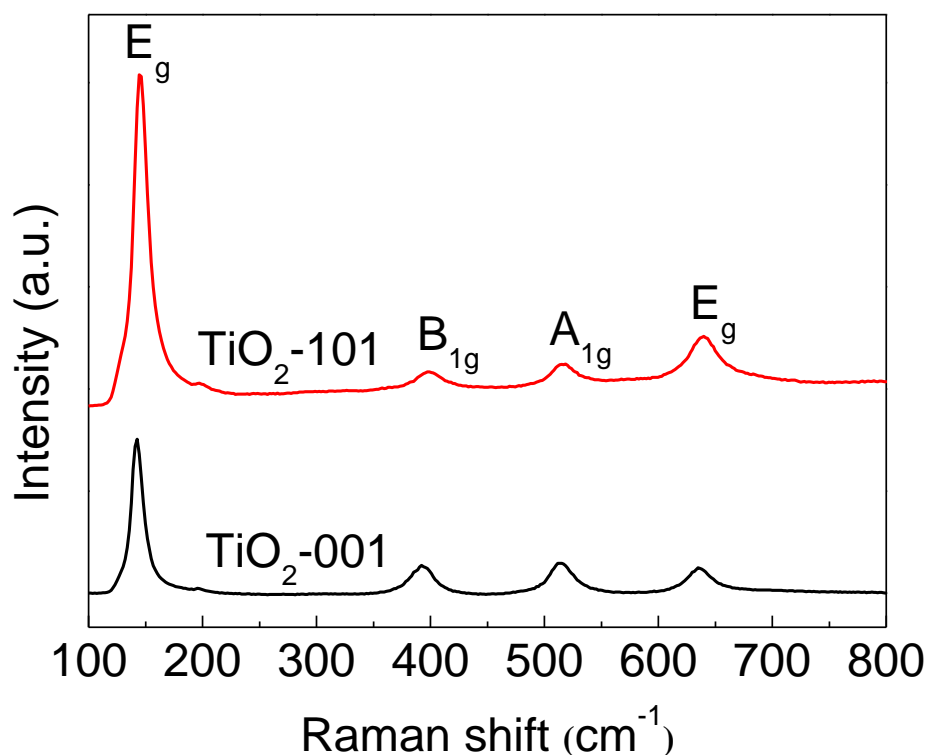


Fig.S1 Raman spectra of TiO_2 nanoparticles

Fig.S1 displayed Raman spectra of TiO_2 nanoparticles. Both samples were of the similar peaks appearing at 144, 394, 514, 636 cm^{-1} , but their intensities varied significantly. It is indicated the typical anatase TiO_2 phase and was also in agreement with the XRD results. E_g peaks at 144 and 636 cm^{-1} were ascribed to the symmetric stretching vibration of O-Ti-O; while the B_{1g} peak at 394 cm^{-1} and A_{1g} peak at 514 cm^{-1} represented the symmetric and anti-symmetric bending vibrations of O-Ti-O, respectively. However, the intensity of the E_g peak in the $\text{TiO}_2\text{-001}$ sample weakened significantly, mainly because of the selective exposure of the $\{001\}$ facets. The $\{001\}$ facet is terminated with unsaturated five-fold Ti atoms (Ti_{5C}) and two-fold O atoms (O_{2C})¹, which weakened the symmetric stretching vibration of O-Ti-O. This result further confirms the preferential exposure of the $\{001\}$ facets on the TiO_2 nanosheets.

According to Wulff Construction, the schematic ideal crystal models of $\text{TiO}_2\text{-101}$ and $\text{TiO}_2\text{-101}$ were shown in Fig.S2(a) and Fig.S2(b), respectively. The proportion of each could be calculated by the following formulae:

$$P_{001} = \frac{S_{001} \times 2}{S_{001} \times 2 + S_{101} \times 8} \times 100\% \quad \text{and} \quad P_{101} = \frac{S_{101} \times 8}{S_{001} \times 2 + S_{101} \times 8} \times 100\%$$

In our cases, the geometrical parameters of the two TiO₂ nanocrystals could be easily obtained from the TEM results, which provide the opportunity to do such a calculation. As a results, the percentages of {101} facets and {001} facets in TiO₂-101 nanospindles are 89% and 11%, while those in TiO₂-001 nanosheet are 23% and 77%, respectively.

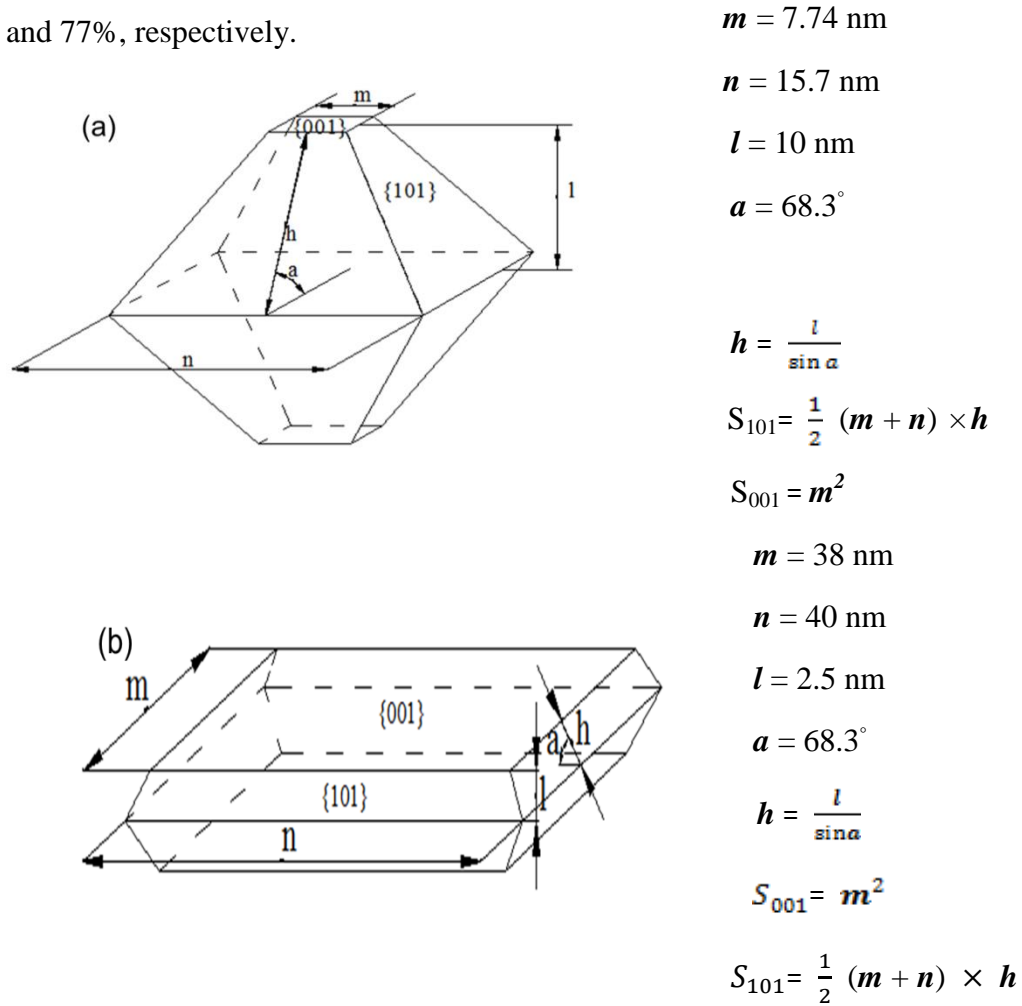


Fig.S2 Ideal crystal models of (a) TiO₂-101 and (b) TiO₂-001

References about the Wulff construction and related calculations are from Ref.2-4.

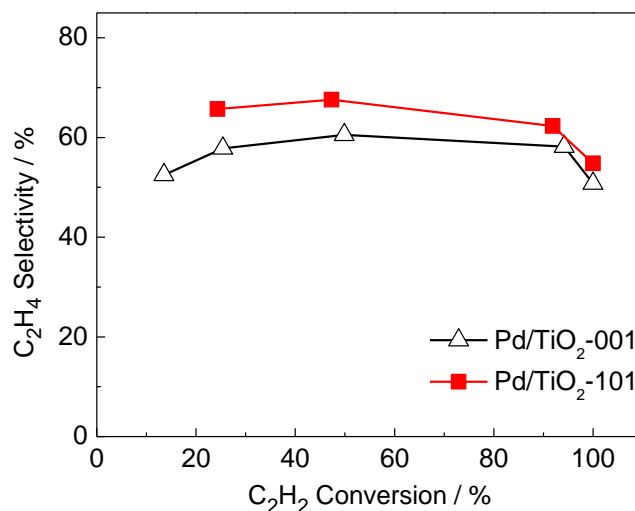


Fig.S3 Ethylene selectivity *versus* acetylene conversion over Pd/TiO₂-001 and Pd/TiO₂-101 catalysts at a total flow rate of 50 mL·min⁻¹ with varying reaction temperatures from 40 to 80 °C

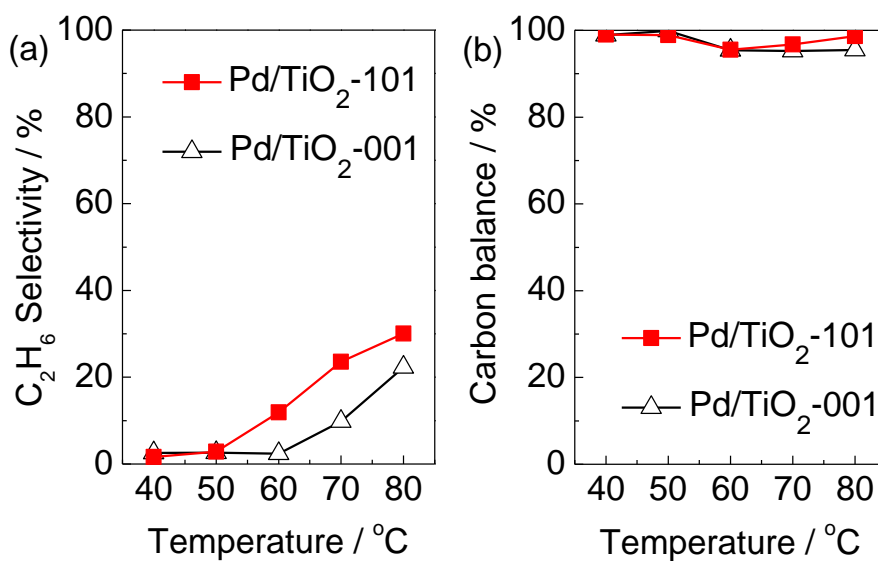


Fig.S4 Selectivity to ethane (a) and the carbon balance (b) *versus* temperature over Pd/TiO₂-001 and Pd/TiO₂-101 catalysts at a total flow rate of 50 mL·min⁻¹ with varying reaction temperatures from 40 to 80 °C

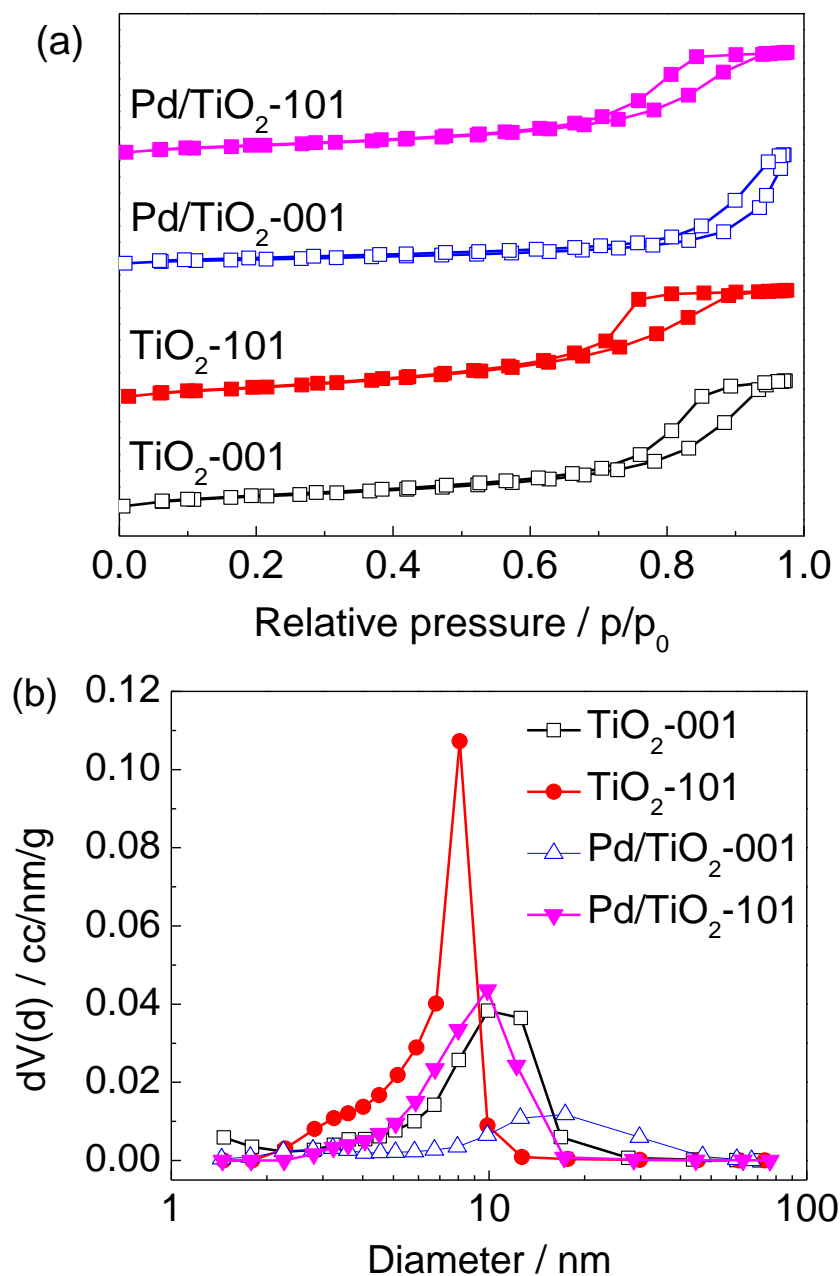


Fig.S5 (a) Nitrogen adsorption-desorption isotherms, and (b) BJH pore-size distributions

Table S1 Summary of physical properties of TiO₂ nanoparticles and Pd/TiO₂ catalysts

Sample	Surface area/(m ² ·g ⁻¹)	Pore volume/(cm ³ ·g ⁻¹)	Pore diameter/nm
TiO ₂ -001	93	0.3127	13.38
1%Pd/TiO ₂ -001	51	0.2698	21.34
TiO ₂ -101	124	0.2757	8.887
1%Pd/TiO ₂ -101	89	0.2590	11.59

References

- (1) Yang, H. G.; Sun, C. H.; Qiao, S. Z.; Zou, J.; Liu, G.; Smith, S. C.; Cheng, H. M.; Lu, G. Q. *Nature* **2008**, *453*, 638. doi: 10.1038/nature06964
- (2) Maitani, M. M.; Tanaka, K.; Mochizuki, D.; Wada, Y. *J. Phys. Chem. Lett.* **2011**, *2*, 2655. doi: 10.1021/jz2011622
- (3) Barnard, A. S.; Curtiss, L. A. *Nano Lett.* **2005**, *5*, 1261. doi: 10.1021/nl050355m
- (4) Liu, L.; Gu, X.; Cao, Y.; Yao, X.; Zhang, L.; Tang, C.; Gao, F.; Dong, L. *ACS Catal.* **2013**, *3*, 2768. doi: 10.1021/cs400492w